International Journal of Sustainable and Green Energy
2014; 3(6): 123-131
Published online November 20, 2014 (http://www.sciencepublishinggroup.com/j/ijrse)
doi: 10.11648/j.ijrse.20140306.12

Initial field testing of concentrating solar photovoltaic (CSPV) thermal hybrid solar energy generator utilizing large aperture parabolic trough and spectrum selective mirrors

Jonathan Richard Raush*, Terrence Lynn Chambers

Department of Mechanical Engineering, University of Louisiana at Lafayette, Lafayette, U. S. A.

Email address:
jrr1239@louisiana.edu (J. R. Raush), tlchambers@louisiana.edu (T. L. Chambers)

To cite this article:
Jonathan Richard Raush, Terrence Lynn Chambers. Initial Field Testing of Concentrating Solar Photovoltaic (CSPV) Thermal Hybrid Solar Energy Generator Utilizing Large Aperture Parabolic Trough and Spectrum Selective Mirrors. *International Journal of Sustainable and Green Energy*. Vol. 3, No. 6, 2014, pp. 123-131. doi: 10.11648/j.ijrse.20140306.12

Abstract: The University of Louisiana at Lafayette has completed initial field testing of a test unit of the MH Solar Concentrating Solar Photovoltaic (CSPV) system. The CSPV unit is a retrofit system for use with a parabolic trough type concentrating solar power (CSP) thermal solar collector which redirects a portion of the incident solar radiation spectrum to a PV module while allowing normal operation of the thermal system to continue. The system was tested at the UL Lafayette Solar Energy Laboratory utilizing the existing Large Aperture Trough (LAT) test field. The dichroic cold mirror reflected solar radiation of between 500 and 1000 nm to the MH Solar vertical multi junction (VMJ) silicon PV cells (known as the MIH VMJ cells) which provided high efficiency operation under a concentration ratio of 30. The testing produced a PV module efficiency of 30% across the portion of the spectrum which was redirected, while the thermal efficiency was reduced by only about 9 percentage points, resulting in an overall efficiency increase of the power plant. The total power output of the power plant could therefore be increased through utilization of the hybrid configuration.

Keywords: Solar Energy, Concentrating Solar Power, CSP, Photovoltaic, CPV-T, CSPV, Hybrid

1. Introduction

For solar energy technologies to reach full market penetration, continued improvements must be made in order to lower the levelized cost of electricity (LCOE) of primary solar energy technologies, including both photovoltaics (PV) and concentrating solar thermal power (CSP). According to the U.S. Department of Energy SunShot Initiative, which proposes a goal of $.06/kWh LCOE for solar energy technologies by the year 2020, a market share of 14% of total U.S. electric production would be reached by 2030 [1]. Current LCOE figures for utility scale projects range from about $0.11/kWh for utility scale PV to $0.13/kWh for utility scale CSP [2]. In an effort to improve overall plant efficiency, and thus drive down LCOE, significant interest has been directed toward the subject of hybrid solar collector systems, integrating multiple receivers and technologies in order to more fully leverage the breadth of the solar radiation spectrum. Differing techniques for hybrid systems have been investigated since as early as the middle of the 20th century, including those which combine PV and photo-thermal (PT) energy conversion in parallel by incorporating spectral beam splitting technologies [3]. Since PT energy conversion processes tend to convert solar energy to thermal energy at efficiencies that maintain relatively constant over the solar spectrum, depending on the optical properties of the thermal receiver, beam-splitting allows the portion of the spectrum that is most advantageous for the PV cell, which is extremely wavelength dependent, to be directed to the cell, while the remaining spectrum can proceed to a thermal receiver for conversion to thermal energy, as in Figure 1 [4].

PV cells are most efficient when converting photons of energies close to the PV cell band-gap energy. Photons below this energy pass through the active area of the cell without being absorbed, and are dissipated as heat. Photons of energy larger than the band are partly utilized, with the remainder of their energy also dissipated as heat. Because of these limitations, a more optimal method of using solar cells would be to direct onto them only the part of the solar spectrum for which high conversion efficiency can be achieved, and to

recover the radiation outside this range by diverting it to a second receiver, which could operate as a thermal, chemical, or different PV band-gap receiver. The concept of a PV-thermal solar hybrid system is that the incident beam is split into PV and thermal spectral components and directed to their respective receivers for conversion to electricity and thermal energy more efficiently.

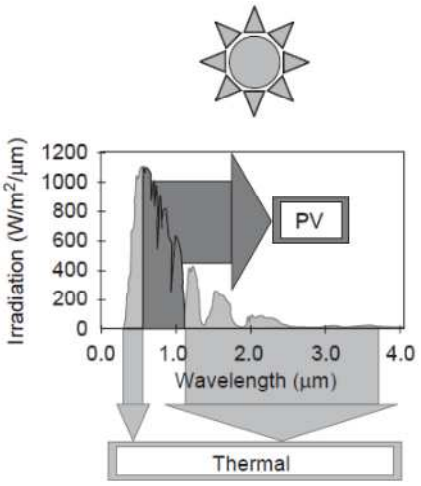

Figure 1. *Spectral filtering for hybrid solar energy production [4].*

Hybrid solar energy systems of various configurations have been proposed, through the inclusion or omitting of various forms of tracking, concentrating, beam splitting, and thermal receivers, in search for the optimal configuration to most completely leverage the given solar resource [5], [6], [7], [8],[9]. Tracking and concentrating PV-thermal hybrid systems are undergoing investigation due to the increased efficiency of some PV cells while under concentration and the cost savings of reducing the area of solar cell needed [10], [11],[12]. Much of this interest also evolves from the deleterious effect of increased temperature on the efficiency of CPV cells, creating a need for efficient thermal management through active heat removal or passive cooling of the cells [13]. Concentrating photovoltaic systems produce the advantage of high efficiency cells but also the complication of decreasing efficiencies with temperature increases. The spectral beam splitting alleviates much of this complication by allowing the longer wavelength radiation to travel directly to the PT device, decreasing the temperature gain and the need for active cooling [6]. Various configurations have been proposed in the literature for both commercial and residential applications, and producing a wide range of theoretical system efficiencies (solar-to-electric), ranging from 10% to upwards of 40%, although few economic estimates are available due to the lack of empirical testing of pilot scale systems.

Kosmadakis, Manolakos, and Papadakis proposed a hybrid system directly coupling a tracking parabolic concentrator with a silicon cell PV system with 10 suns concentration, and an organic Rankine cycle (ORC) thermal power generator. The full solar spectrum was directed to the PV cell with the thermal system acting as a heat sink. A numerical optimization concluded that the CPV–ORC combination improved the efficiency of CPV technology from 9.81% to 11.83% [14]. Liu, Hu, Zhang, and Chen proposed a hybrid system utilizing a two-axis tracking Fresnel concentrator with beam splitter and a secondary parabolic reflector and crystal silicone PV cells [15]. A numerically evaluated efficiency gain from 22.9% for the CPV system alone to 26.5% for the hybrid system was reported for cell operating temperature of 25 ^{o}C and from 19.8% to 25.6% for cell operating temperature of 50 ^{o}C. Ju, Wang, Flamant, Li, and Zhao proposed a hybrid system utilizing a Fresnel concentrator with beam splitter coupled with a gallium arsenide (GaAs) solar cell and a $CoSb_3$ thermo-electric generator. Analyzed numerically, the proposed system generated an optimal system efficiency of 26.62% and 27.49%, corresponding to heat sink heat transfer coefficients of 3000 W/m^{2}K and 4500 W/m^{2}K, respectively[16]. The concentration ratio ranged from 550 to 770 suns.

Many of the recent investigations involving CSPV hybrid systems focus on the triple junction solar cell configuration, which when utilizing the full solar spectrum would operate at a higher theoretical efficiency than single crystalline silicon and other solar cell chemistries [12]. Chen et al, described a two-axis tracking concentrator focusing the full solar spectrum to a triple junction solar cell module coupled with a thermal energy collection system. The cell consisted of a top cell of InGaP, middle cell InGaAs and bottom cell Ge, connected in series. The system produced a solar cell efficiency of 26% while maintaining a thermal conversion efficiency of 52% [17].

2. Background and System Description

The University of Louisiana at Lafayette (UL Lafayette) has completed the initial field testing of a concentrating solar photovoltaic (CSPV) hybrid solar power system utilizing a vertical multi junction (VMJ) cell developed by MH Solar Co., Ltd. (MH Solar) - the MIH VMJ cell (VMJ cell). The parabolic trough CSPV system produces thermal energy by way of traditional concentrating solar power through the existing heat collection element (HCE) tubes, while producing electricity directly from a concentrating PV system operating in parallel. This is accomplished by splitting the solar radiation beam, filtering out the spectrum of wavelengths that are most efficiently converted to electricity by the silicon PV cells and redirecting the light onto the PV module, while leaving the remaining ultraviolet and infrared light to pass to the existing thermal receiver of the parabolic trough. This type of hybrid system, utilizing a single axis linear concentrator, a solar radiation beam splitter, and linear thermal receiver has been proposed previously [18]. However, the MH Solar system cell technology applies a novel VMJ cell which makes it uniquely suitable for this application.

The MIH VMJ cell is produced by stacking and bonding together a large number of P-N diffused silicon wafers, which is then cut vertically into thin MIH VMJ cells. This process has several distinct advantages to other CPV cell configurations. Because each P-N junction is in series, the MIH VMJ cell can generate a very high voltage in a small

package. Each additional wafer added to the stack adds another 0.6V to the total device voltage, resulting in less current for a given solar cell area [19]. In addition the modules are easily scalable in size and output voltage. The parabolic trough CSPV application requires a solar cell that can perform well with moderate to high solar concentration, as well as under a partial solar spectrum. Similar to a triple junction solar cell, the MIH VMJ cell performance improves when in concentrated sunlight, and was shown to have linear performance out to 2500 suns concentration [15]. However, unlike triple junction cells which rely on the full solar spectrum for high efficiency operation, the MIH VMJ cell operates at peak efficiency within the spectral range most optimal for hybrid applications. According to Imenes and Mills, the band-pass region of the beam splitter for silicon cells is from 590 to 1082 nm for the optimization of peak electrical output when combined with a thermal receiver [4]. Filtering this spectral band from the rest of the spectrum and directing it to silicon cells results in relatively high electrical conversion efficiencies such as 30% relative to the total solar energy of the spectral band [5]. The MIH VMJ cell displays peak solar conversion efficiencies within this range of the solar spectrum, while a triple-junction solar cell's performance will drop dramatically when illuminated by only a part of the solar spectrum, as shown in Figures 2 and 3 [20].

Additionally, the MIH VMJ cell's performance is reduced by only 3% for every 10 ^{o}C operation above its standard test conditions (Figure 4) [19]. This performance loss is not as dramatic as conventional silicon solar cells, which can lose 5% in performance for every 10 ^{o}C temperature rise [13].

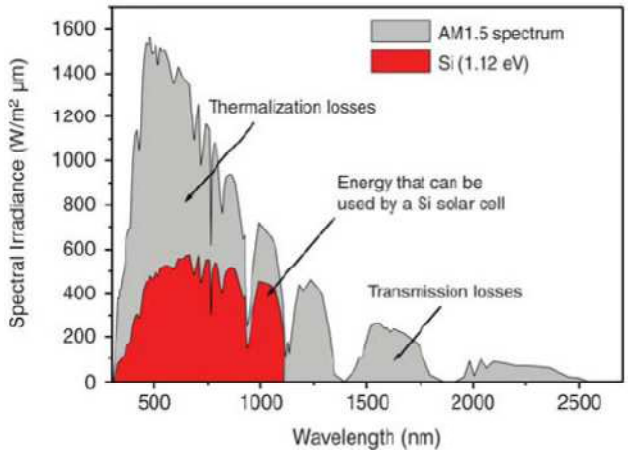

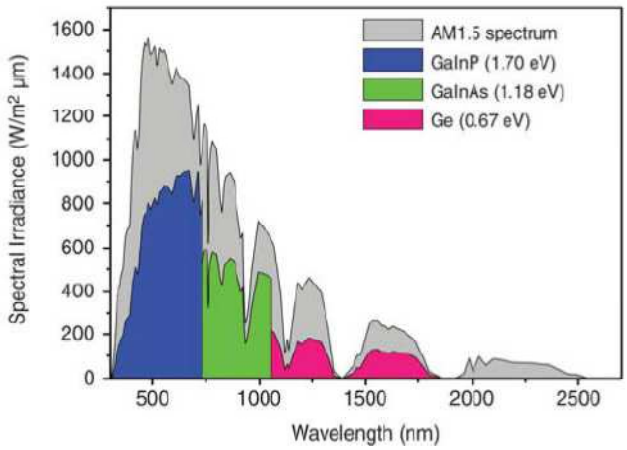

Figures 2 and 3. *The AM1.5 solar spectrum and the parts of the spectrum that can be used by: Si solar cells (left figure) and certain triple junction solar cells (right figure) [20].*

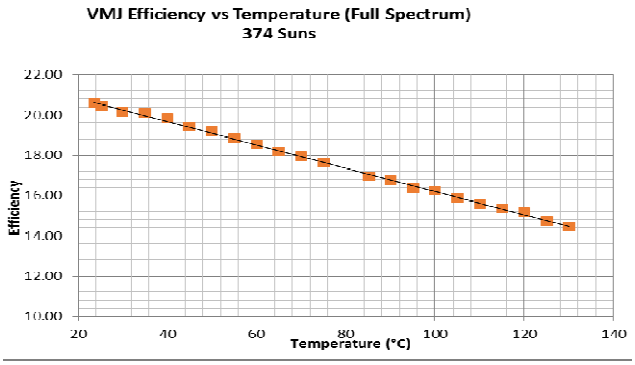

Figure 4. *MIH VMJ cell efficiency vs. temperature. Courtesy of MH Solar.*

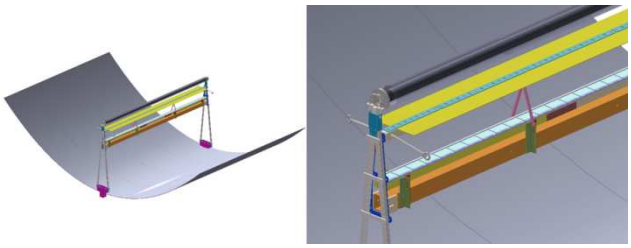

Figures 5 and 6. *Depiction of CPV unit with cold mirrors and MIH VMJ cells. Courtesy of MH Solar.*

3. Test Platform

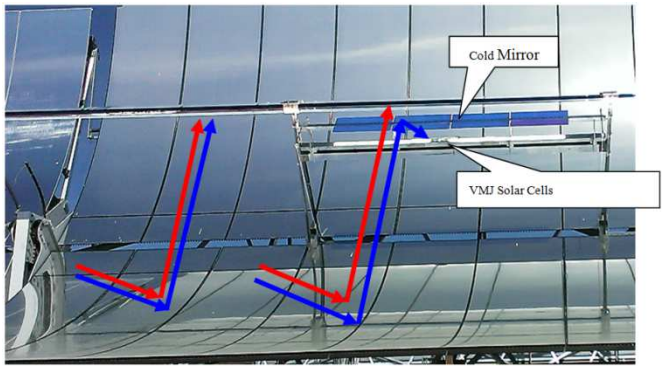

Figure 7. *Schematic depiction of dichroic cold mirror operation. Red arrows represent infrared light; blue arrows represent visible light.*

The VMJ cells were placed linearly in parallel with the HCE tube and with rotatable mirrors installed to either supply all of the incident solar radiation to the HCE tube while stowed, or to provide a selected spectrum of radiation to the cells while deployed. Depicted in Figures 5 and 6, the solar cells are passively cooled by use of a heat sink to ambient temperature. A depiction of the cold mirror operation in Figure 7 demonstrates the operation of the beam splitting "cold

mirror", which reflects the visible portion of the spectrum (blue arrows) while allowing most infrared wavelengths (red arrows) to be transmitted efficiently. The cold mirror was a dichroic spectrally selective mirror with the dichroic film by Evaporated Metal Films Corporation (EMF). The cold mirror demonstrated excellent spectral reflectance in the band of 500 to 1000 nm as seen in Figure 8, while also demonstrating good transmittance outside of this band (Figure 9), presented here on a low iron glass substrate.

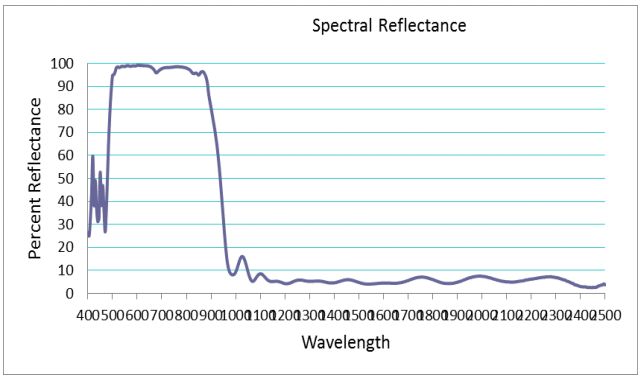

Figure 8. *Spectral reflectance of dichroic cold mirror.*

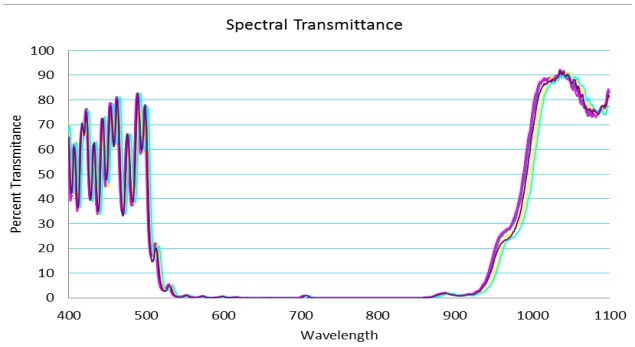

Figure 9. *Spectral transmittance of dichroic filter.*

Testing was conducted at the UL Lafayette Solar Technologies Application, Research and Testing (START) Center, where the only operating solar thermal power plant in Louisiana is located [21]. The CSPV module was installed on a Large Aperture Trough (LAT) from Gossamer Space Frames. The parabolic trough had an aperture of 7.3 meters and was oriented in a North-South configuration, while tracking from East to West. The thermal receiver was the PTR70, 70 mm heat collection element (HCE) tube from Schott. Previous testing completed by UL Lafayette has demonstrated direct normal (DNI) solar-to-thermal efficiencies of the solar collector in the range of 70 to 80 percent under optimum conditions [22]. Solar radiation measurements were taken onsite by the Kipp & Zonen SOLYS 2 Sun Tracker and CHP 1 pyreheliometer system. The LAT collector field consisted of 12 individual troughs, each 12 m in length arranged into two Solar Collector Assemblies (SCAs) (Figure 10). The collector field was coupled to an organic Rankine cycle (ORC) thermal power plant. Additional key metrics of the UL Lafayette solar thermal test facility are listed in Table 1.

Figure 10. *Representation of UL Lafayette START Center.*

Table 1. *Plant characteristics.*

Plant Location	**Crowley, LA**
Yearly Direct Normal Solar	1590 kWh/m^2
Plant Size (nominal)	50 kWe
ORC Gross Output	50 kWe
Solar Field Heat Transfer Fluid	Water
Inlet Temperature	93˚C
Outlet Temperature	121˚C
ORC Working Fluid	R245fa
ORC Design Point Efficiency	8%
Solar Field Size	1051 m^2
Land Area	4050 m^2 (1 acre)
Solar to Electric Design Point Efficiency	6%

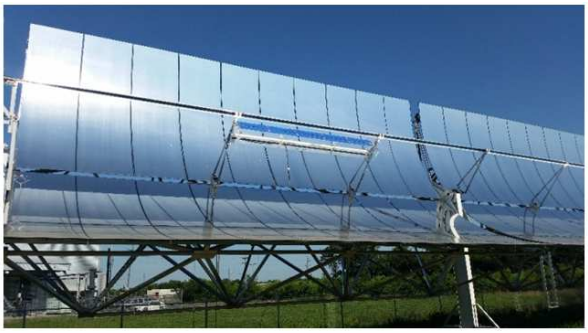

Figure 11. *MH Solar CSPV system installed at the UL Lafayette START Center.*

For the testing conducted at the UL Lafayette testing facility, one MH Solar module was installed in parallel with the HCE tube, four meters in length, on one parabolic trough Solar Collector Assembly (SCA) section (Figures 11 and 12). The focal length of the HCE tube was 2.0 m, and the cold mirrors, six inches in width, were placed at a distance 260 mm from the mirror surface, intercepting about 29 percent of the reflected light, according to the ray trace conducted by MH Solar. The mirror substrate was 3.2 mm thick glass. Both borosilicate float glass and low iron glass as the mirror substrate were tested. Additional key metrics of the PV module are listed in Table 2. The test plan included the operation of the CSPV system both with traditional full spectrum mirrors as well as the cold mirrors in both the deployed and stowed configuration.

Figure 12. *MH Solar CSPV system installed at the UL Lafayette START Center.*

Table 2. *PV cell module characteristics.*

Cell width	2 cm
Cell length	5.5 cm
Area of the cell, A_{cells}	11 cm^c
Cells/Module	6
How many cells wide (per module)	3 cells
Packing Density (length)	92%
Packing Density (width)	97%
Overall packing density	88.9%
Module Length	12.0 cm
Module's / m	8.4
Module's / Trough	100

4. Results

Experimental data was collected in an effort to quantify the effect of the CSPV module on the overall efficiency of the parabolic trough collector field. The solar radiation conversion efficiencies were calculated based on measured data for both the PV module and the thermal receiver to determine system performance.

4.1. PV Performance Data

Power and efficiency calculations of the MIH VMJ cells could be completed by use of the voltage and current measurements taken during operational testing of the cells under the concentrated and spectrally selective conditions described above. Open circuit voltage and short circuit current readings for two tests are given in Table 3. Here I_{sc} (900) is the short-circuit current normalized to a DNI of a standard test condition of 900 W/m^2. The conversion efficiency η_{PV} of the cell module is defined as:

$$\eta_{PV} = \frac{P_{PV}}{q_{PV}} \quad (1)$$

where P_{PV} is the power generated by the cell module and q_{PV} is the solar energy incident on the cell module. The solar energy delivered to the cells can be expressed as:

$$q_{PV} = q_{in} * \eta_{CM} * \int_0^{\infty} \rho(\lambda) d\lambda * \eta_{\tau,cell} * \gamma_{cells} \quad (2)$$

where q_{in} is the incident solar radiation onto the trough, $q_{solar,}$ multiplied by an adjustment factor due to the cosine effect, $\cos(\theta)$ [23],

$$q_{in} = q_{solar} * \cos(\theta) . \quad (3)$$

In (2), η_{CM} is the efficiency of incident radiation reaching the cold mirror, $\rho(\lambda)$ is the spectral reflectivity of the cold mirror, $\eta_{\tau,cell}$ is the transmission efficiency of the cell module cover glass, and γ_{cells} is the packing density of the cells in the module. In order to determine q_{PV} a DNI of 900 W/m^2 was assumed as a standard test condition. The fraction of light reaching the cold mirror was determined from:

$$\eta_{CM} = A_{trough} * \eta_{opt} * \eta_{soiling} * \eta_{CM\ intercept} * \eta_{shading} \quad (4)$$

where A_{trough} is the area of the parabolic trough per unit PV module, η_{opt} is the optical efficiency of the trough mirror, $\eta_{soiling}$ is the soiling factor of the trough mirror, $\eta_{CM\ intercept}$ is the fraction of trough aperture intercepted by the cold mirror, and $\eta_{shading}$ is the shading factor on the trough by the PV module, the latter two being determined by a ray trace conducted by MH Solar. The factors mentioned above relating to the testing conducted are listed in Table 3.

The power generated by the PV module, P_{PV} can be expressed as [15]:

$$P_{PV} = A_{cells} * V_{OC} * I_{SC} * FF \quad (5)$$

where A_{cells} is the area of the PV cells, Voc is the open-circuit voltage, I_{sc} is the short-circuit current density and *FF* is the fill factor. The open-circuit voltage and short-circuit current measurements for two tests are listed in Tables 4 and 5, along with the max power, normalized to a DNI of 900 W/m^2. Also listed are additional test conditions including the actual DNI at the time of measurement. Figure 13 depicts the fill factor measurements at a concentration of 374 suns versus temperature. An empirically measured fill factor of 0.75 is utilized for the efficiency analysis (Figure 14).

Table 3. *PV cell and cold mirror characteristics.*

Aperture Width	**7.3 m**
Module length	**0.12 m**
A_{trough}	0.876 m^2
q_{in}	900 W/m^2
η_{opt}	85%
$\eta_{soiling}$	95%
$\eta_{CM\ intercept}$	29%
$\eta_{shading}$	96%
γ_{cells}	88.9%
ρ (total)	48.6%
$\eta_{\tau,cell}$	90%

For the given results of Test 1 an average power produced per module was 20.05 Watts, with a of 69 Watts, resulting in a PV efficiency of 29% under the spectrally selective and concentrated conditions. The second set of tests yielded a PV efficiency of 29.5%. This efficiency calculation is dependent on an accurate optical efficiency calculation not available at the time of the test and therefore Table 5 is given which illustrated the range of efficiencies based on potential optical efficiency corrections.

Table 4. *Test 1 results.*

Reading - 1				**Reading - 2**			
V_{oc} (V)	**I_{sc} (mA)**	**I_{sc}(900)**	**P_{max}(900)W**	**V_{oc} (V)**	**I_{sc} (mA)**	**I_{sc}(900)**	**P_{max}(900)W**
260.80	80.00	100.42	19.66	250.30	80.00	105.57	19.84
261.10	82.20	103.18	20.23	251.40	82.20	108.48	20.47
Time	3:58			4:01			
DNI	717			682			
Ambient Temp.	86.0			86.0			
Mirrors Used	low iron, 3.2mm cold mirror			low iron, 3.2mm cold mirror			
cosine correction	0.999			0.999			

Table 5. *Test 2 results*

Reading - 1				**Reading - 2**			
Voc (V)	**Isc (mA)**	**Isc(900)**	**Pm(900)W**	**Voc (V)**	**Isc (mA)**	**Isc(900)**	**Pm(900)W**
256.70	86.70	112.27	21.79	251.10	86.60	106.33	20.19
256.60	81.10	105.02	20.37	250.30	81.10	99.58	18.84
Time	4:20			4:23			
DNI	695			733			
Ambient Temp.	84.0			84.0			
Mirrors used	boro float, 3.2mm cold mirror			boro float, 3.2mm cold mirror			
Cosine correction	0.992			0.992			

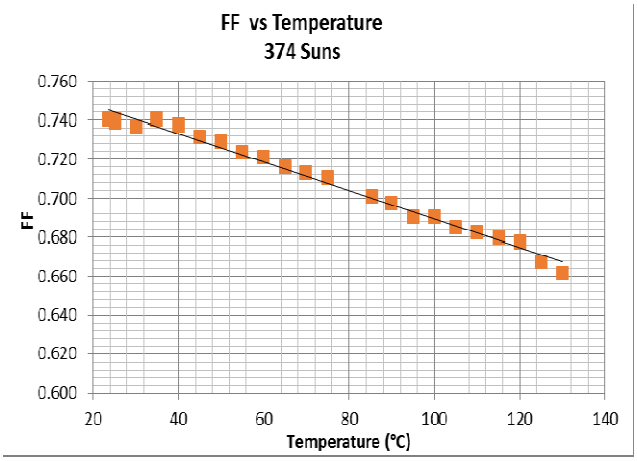

Figure 13. *Fill factor vs. temperature for concentration ratio of 374.*

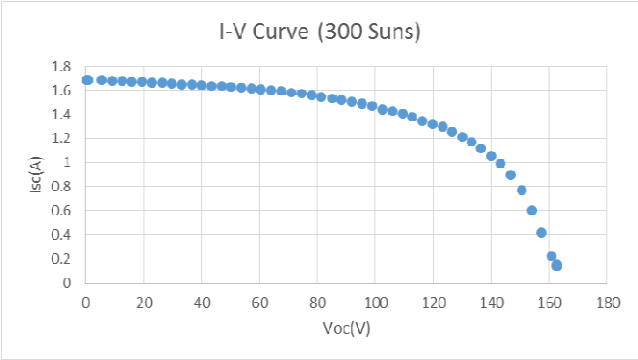

Figure 14. *I-V curve for concentration ratio of 300.*

Table 6. *Range of MIH VMJ cell efficiencies based on various optical efficiencies.*

	Optical Efficiency								
Cell Efficiency	**78 %**	**79 %**	**80 %**	**81 %**	**82 %**	**83 %**	**84 %**	**85 %**	**86 %**
29.0%									
29.5%									
30.0%									
30.5%									
31.0%									
31.5%									
32.0%									
32.5%									
33.0%									
33.5%									

4.2. Thermal Performance Data

The thermal efficiency, η_T, of the solar collector field can be expressed as:

$$\eta_T = \frac{P_T}{q_{in}} \tag{6}$$

where P_T is the thermal power generated by the solar field. The thermal power is calculated from the process flow data of the HTF through the collector field:

$$P_T = \dot{m} \int_{T_{in}}^{T_{out}} C_p dT \tag{7}$$

where $\dot{m}$ is the mass flow rate of the heat transfer fluid through the solar collector field, C_p is the specific heat of constant pressure, and T_{in} and T_{out} are the temperatures of the HTF leaving and entering the collector field, respectively. For the testing described here, the HTF was water with a 10 percent glycol mixture. Over the temperature ranges utilized in this study, the specific heat could be considered constant, resulting in:

$$P_T = \dot{m} C_p \Delta T \quad (8)$$

where ΔT is the temperature gain through the collector field. The temperature gain through the portion of the parabolic trough which contained the cold mirrors, 4 meters in length, was examined. The ΔT was recorded for conditions without the CSPV mirrors installed, with the mirrors installed but stowed, and with the mirrors installed and deployed. A measurement was also recorded with full spectrum mirrors deployed in the place of the cold mirrors. In order to compare the effect on thermal performance with the CSPV cold mirrors in use, the thermal efficiency of the solar collector field was determined for each case and the difference taken. For the full mirrors, an average difference in thermal efficiency of 2.4 percentage points was observed during testing for deployed and stowed. Figure 15 depicts the results from one such test. The efficiency in both the stowed and deployed positions trended upward during the test day due to changes in tracking error which occur in normal operation. The tracking error typically maintains a 0.05 degree tolerance to the calculated sun angle. The absolute value of the tracking error for the test day is depicted in Figure 16. This fluctuation in tracking accuracy therefore accounts for some of the fluctuation seen in the efficiency calculations. Figure 17 displays the cosine corrected DNI during the CSPV test with the full mirrors in place.

In terms of efficiency, the deployed full mirror intercepted 29% of the aperture of a 4 meter linear distance, or 1/9th of the span where the efficiency calculation occurred. Therefore, considering the full 36 meter length (1/2 SCA) where the temperature measurements were taken, the expected measured reduction in efficiency across the span would be $\frac{1}{9} * 29\% = 3.2\%$ of the unobstructed thermal efficiency. During this testing, the unobstructed thermal efficiency was about 70.5%. A 3.2% reduction in efficiency would result in a drop of 2.25 percentage points, which is close agreement with the 2.4 point drop in thermal performance as measured in this testing. By applying the measured loss of efficiency across the full ½ SCA, the total reduction in efficiency of a fully equipped section (9 CSPV modules) would be 9*2.4 = 21.6 points while the full mirrors were deployed. This is in good agreement with the estimated 29%*70.5% = 20.5 percentage point reduction that would be expected.

The cold mirrors were tested utilizing a low iron glass substrate, resulting in an average difference in thermal efficiency of 1.03 percentage points, or 1.6 % reduction in efficiency. Figure 18 depicts results of the cold mirror testing. Comparing to the full mirror, this result would suggest that about 45.5% of the radiation spectrum successfully passed through the cold mirror. This compares to the expected 48.6% of the spectrum to be reflected. Extending the thermal efficiency reduction from the cold mirror across the full length of the span (1/2 SCA) in which the temperature measurements were taken results in a 9.3 reduction in percentage points, or 14%, reduction in thermal efficiency. Figure 19 shows the cosine corrected DNI during the CSPV test with the cold mirrors.

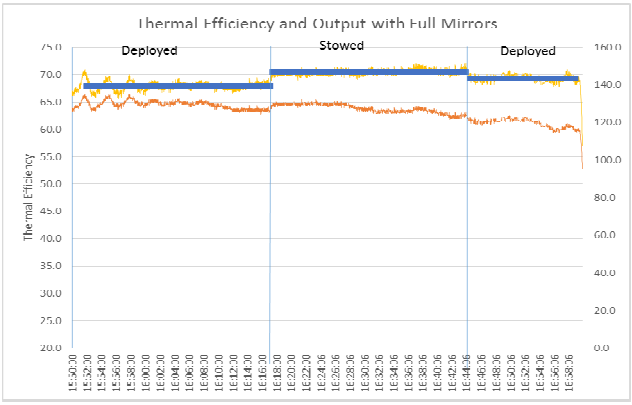

Figure 15. *Thermal efficiency of CSPV system with full mirrors in deployed and stowed condition.*

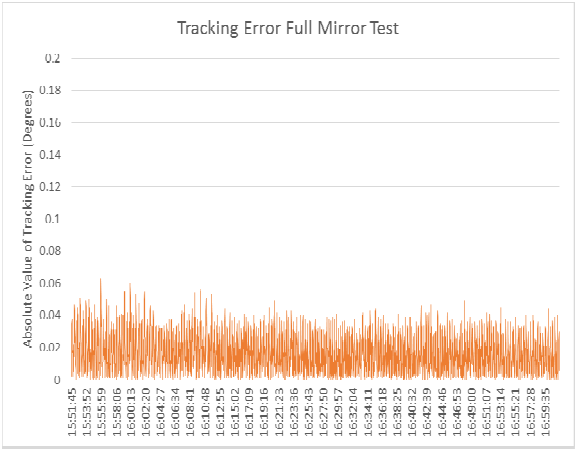

Figure 16*. Absolute value of tracking error during CSPV test with full mirror.*

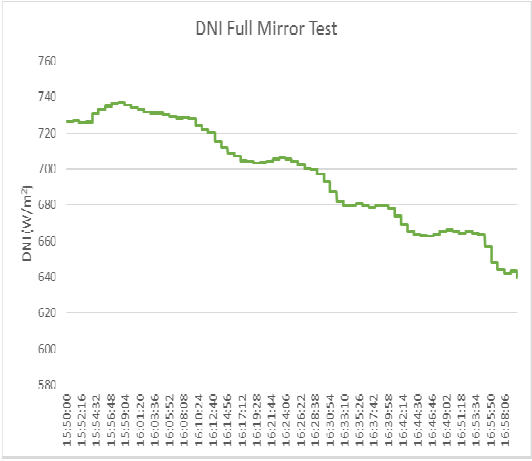

Figure 17. *Cosine corrected DNI during CSPV test with full mirrors.*

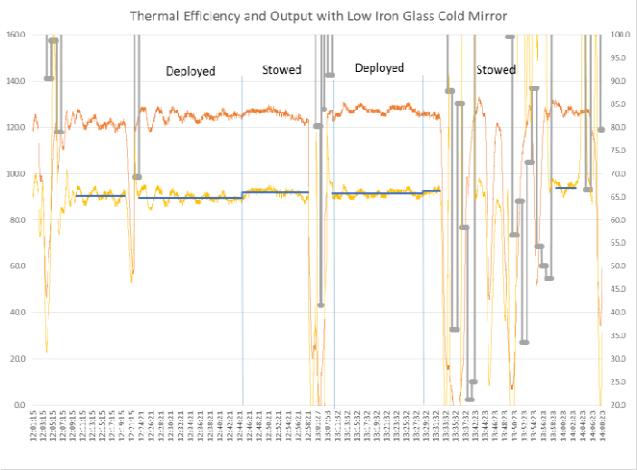

Figure 18. *Thermal efficiency of CSPV system with cold mirrors in stowed and deployed position.*

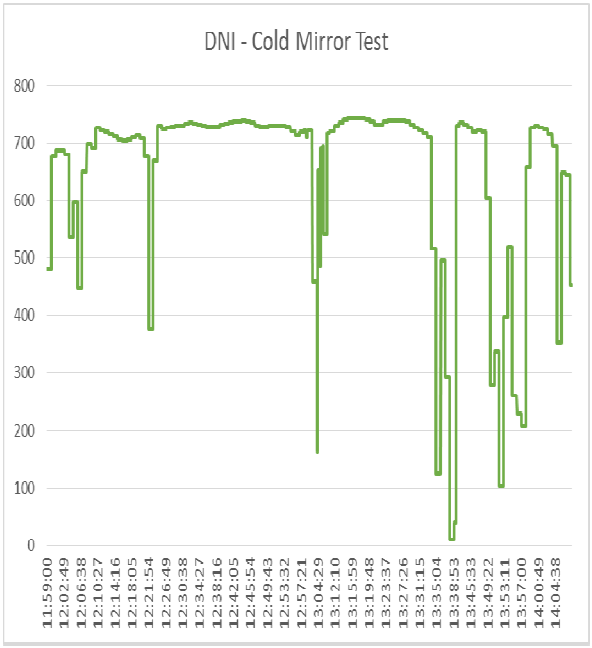

Figure 19. *Cosine corrected DNI curing CSPV test with cold mirrors.*

The system efficiency, η_{system}, with the PV and thermal systems operating in parallel can be express as

$$\eta_{system} = \frac{P_{system}}{q_{in}} \tag{9}$$

where P_{system} is the system power found from:

$$P_{system} = P_{PV} + P_{thermal} \tag{10}$$

Using the results from the PV tests in Table 3, given a DNI of about 715 W/m^2, an additional 541 W of power are added to the system from the 4 m span. There are 9 four-meter spans in the area of the collector field under investigation, resulting in a total addition of 4,870 W of electric power. In order to determine the overall change in power output of the solar collector field, the thermal energy was assumed to be converted to electricity at an efficiency of between 33% and 35%, which is typical of installed parabolic trough solar thermal power plants, excluding any natural gas supplement [24]–[27]. Based on the assumed conversion rate and using the thermal data when the DNI was 715 W/m^2, a total of between 42,160 W and 44,420 W of electric power would be produced from the area of collector field under investigation (half of one SCA), 263 m^2 of aperture area. This compares to between 40,854 W and 43,330 W of electric power without the CSPV installation, resulting in an overall increase of 2.5% to 3.2% of power output from the solar collector field.

5. Discussion and Conclusions

Initial test results of a CSPV hybrid photovoltaic and thermal solar energy system have been presented. The combination of the CPV performance data and the thermal performance data show an overall increase in system efficiency from the base thermal only case. Based on the testing, an overall system solar-to-electric efficiency improvement from 21.7 percent to 22.5 percent was achieved. This increase in system efficiency was achieved through the employment of the MIH VMJ cell which has a high efficiency within the solar radiation spectrum bandwidth of 500 to 1000 nm. This bandwidth was selectively directed toward the PV portion of the spectrum at a concentration ratio of about 30. This allowed the PV cells to operate at high efficiency while also utilizing passive cooling. The remaining solar radiation spectrum was directed toward the parabolic trough HCE tube at a concentration ratio of 104, efficiently converting the remaining spectrum into thermal energy.

Future work involves conducting longer term additional optical efficiency measurements in order to more accurately determine the actual CPV cell efficiencies. Utilizing lower flow rates will increase the temperature gain through the field and provide higher resolution for data analysis. Additional analysis is needed to determine the optimal operational configuration for the CSPV system. Based on the operating scheme of a particular plant, the advantages built-in to operating the CPV system could be manifested in several ways. One, the operator could utilize the cold mirrors in the full collector field in order to capture the peak solar irradiation that is beyond the design rating of the field and would have been otherwise directed to storage. This could allow optimal generation of electrical power based on peak demand and value of the generated power. An additional scenario would involve using full mirrors to capture the solar irradiation in portions of the collector field that would otherwise have been dumped based on the rated capacity of the thermal power block.

Acknowledgements

This work was supported and made possible by funding from Cleco Power LLC and the University of Louisiana at Lafayette.

References

[1] R. Margolis, C. Coggeshall, and J. Zuboy, "Sunshot Vision Study," *US Dept. Energy*, no. February, 2012.

[2] "Progress Report: Advancing Solar Energy Across America | Department of Energy." [Online]. Available: http://energy.gov/articles/progress-report-advancing-solar-energy-across-america. [Accessed: 01-Aug-2014].

[3] A. Mojiri, R. Taylor, E. Thomsen, and G. Rosengarten, "Spectral beam splitting for efficient conversion of solar energy—A review," *Renew. Sustain. Energy Rev.*, vol. 28, pp. 654–663, Dec. 2013.

[4] A. G. Imenes and D. R. Mills, "Spectral beam splitting technology for increased conversion efficiency in solar concentrating systems: a review," *Sol. Energy Mater. Sol. Cells*, vol. 84, no. 1–4, pp. 19–69, Oct. 2004.

[5] A. Mojiri, C. Stanley, and G. Rosengarten, "Spectrally Splitting Hybrid Photovoltaic/thermal Receiver Design for a Linear Concentrator," *Energy Procedia*, vol. 48, pp. 618–627, 2014.

[6] Y. Li, S. Witharana, H. Cao, M. Lasfargues, Y. Huang, and Y. Ding, "Wide spectrum solar energy harvesting through an integrated photovoltaic and thermoelectric system," *Particuology*, vol. 15, pp. 39–44, Aug. 2014.

[7] F. Shan, F. Tang, L. Cao, and G. Fang, "Performance evaluations and applications of photovoltaic–thermal collectors and systems," *Renew. Sustain. Energy Rev.*, vol. 33, pp. 467–483, May 2014.

[8] V. V. Tyagi, S. C. Kaushik, and S. K. Tyagi, "Advancement in solar photovoltaic/thermal (PV/T) hybrid collector technology," *Renew. Sustain. Energy Rev.*, vol. 16, no. 3, pp. 1383–1398, Apr. 2012.

[9] L. Tan, X. Ji, M. Li, C. Leng, X. Luo, and H. Li, "The experimental study of a two-stage photovoltaic thermal system based on solar trough concentration," *Energy Convers. Manag.*, vol. 86, pp. 410–417, Oct. 2014.

[10] N. R. E. Wilson, Greg; Emergy, Keith; Laboratory, "Best Research-Cell Efficiencies." [Online]. Available: http://www.nrel.gov/ncpv/images/efficiency_chart.jpg. [Accessed: 13-Oct-2014].

[11] E. F. Fernández, G. Siefer, F. Almonacid, A. J. G. Loureiro, and P. Pérez-Higueras, "A two subcell equivalent solar cell model for III–V triple junction solar cells under spectrum and temperature variations," *Sol. Energy*, vol. 92, pp. 221–229, Jun. 2013.

[12] H. Helmers, M. Schachtner, and A. W. Bett, "Influence of temperature and irradiance on triple-junction solar subcells," *Sol. Energy Mater. Sol. Cells*, vol. 116, pp. 144–152, Sep. 2013.

[13] E. Skoplaki and J. a. Palyvos, "On the temperature dependence of photovoltaic module electrical performance: A review of efficiency/power correlations," *Sol. Energy*, vol. 83, no. 5, pp. 614–624, May 2009.

[14] G. Kosmadakis, D. Manolakos, and G. Papadakis, "Simulation and economic analysis of a CPV/thermal system coupled with an organic Rankine cycle for increased power generation," *Sol. Energy*, vol. 85, no. 2, pp. 308–324, Feb. 2011.

[15] Y. Liu, P. Hu, Q. Zhang, and Z. Chen, "Thermodynamic and optical analysis for a CPV/T hybrid system with beam splitter and fully tracked linear Fresnel reflector concentrator utilizing sloped panels," *Sol. Energy*, vol. 103, pp. 191–199, May 2014.

[16] X. Ju, Z. Wang, G. Flamant, P. Li, and W. Zhao, "Numerical analysis and optimization of a spectrum splitting concentration photovoltaic–thermoelectric hybrid system," *Sol. Energy*, vol. 86, no. 6, pp. 1941–1954, Jun. 2012.

[17] H. Chen, J. Ji, Y. Wang, W. Sun, G. Pei, and Z. Yu, "Thermal analysis of a high concentration photovoltaic/thermal system," *Sol. Energy*, vol. 107, pp. 372–379, Sep. 2014.

[18] S. Jiang, P. Hu, S. Mo, and Z. Chen, "Optical modeling for a two-stage parabolic trough concentrating photovoltaic/thermal system using spectral beam splitting technology," *Sol. Energy Mater. Sol. Cells*, vol. 94, no. 10, pp. 1686–1696, Oct. 2010.

[19] B. Sater, M. Perales, J. Jackson, S. Gadkari, and T. Zahuranec, "Cost-effective high intensity concentrated photovoltaic system," *IEEE 2011 EnergyTech*, pp. 1–6, May 2011.

[20] N. Yastrebova, "High efficiency multi-junction solar cells: current status and future potential," University of Ottawa SUNLAB, Ottowa, Canada. [Online]. Available: http://sunlab.eecs.uottawa.ca/?page_id=134. [Accessed 13-Oct-2014].

[21] T. Chambers, J. Raush, and G. Massiha, "Pilot solar thermal power plant station in southwest Louisiana," *Int. J. Appl. Power Eng.*, vol. 2, no. 1, 2013.

[22] J. Raush and T. Chambers, "Demonstration of Pilot Scale Large Aperture Parabolic Trough Organic Rankine Cycle Solar Thermal Power Plant in Louisiana," *J. Power Energy Eng.*, vol. 1, no. 7, pp. 29–39, 2013.

[23] E. Leonardi and B. D'Aguanno, "CRS4-2: A numerical code for the calculation of the solar power collected in a central receiver system," *Energy*, vol. 36, no. 8, pp. 4828–4837, Aug. 2011.

[24] "System Advisor Model (SAM) Case Study :," National Renewable Energy Laboratory, [Online]. Available: https://sam.nrel.gov/content/case-studies. [Accessed 13-Oct-2014].

[25] R. Cable, "Solar Trough Generation - The California Experience," *ASES Forum 2001,* Washington D.C., 2001.

[26] E. F. Camacho and A. J. Gallego, "Optimal operation in solar trough plants: A case study," *Sol. Energy*, vol. 95, pp. 106–117, Sep. 2013.

[27] H. Price, "A Parabolic Trough Solar Power Plant Simulation Model Preprint," ISES 2003, International Solar Energy Conference. National Renewable Energy Laboratory, January, 2003.